Prostatic artery occlusion: initial findings on pathophysiological response in a canine prostate model

Vanesa Lucas-Cava[1]^, Francisco Miguel Sánchez-Margallo[2,3]^, Beatriz Moreno-Lobato[4]^, Luis Dávila-Gómez[5], Juan Rafael Lima-Rodríguez[6]^, Virginio García-Martínez[7]^, Carmen López-Sánchez[7]^, Fei Sun[1,3]^

[1]Endoluminal Therapy and Diagnosis Unit, Jesús Usón Minimally Invasive Surgery Centre, Cáceres, Spain; [2]Scientific Director, Jesús Usón Minimally Invasive Surgery Centre, Cáceres, Spain; [3]CIBER de Enfermedades Cardiovasculares (CIBERCV), Madrid, Spain; [4]Animal Modelling Service, Jesús Usón Minimally Invasive Surgery Centre, Cáceres, Spain; [5]Animal Housing Service, Jesús Usón Minimally Invasive Surgery Centre, Cáceres, Spain; [6]Anaesthesiology Unit, Jesús Usón Minimally Invasive Surgery Centre, Cáceres, Spain; [7]Human Anatomy and Embryology, Faculty of Medicine, University of Extremadura, Badajoz, Spain

Contributions: (I) Conception and design: V Lucas-Cava, F Sun; (II) Administrative support: All authors; (III) Provision of study materials or patients: L Dávila-Gómez, JR Lima-Rodríguez; (IV) Collection and assembly of data: V Lucas-Cava, B Moreno-Lobato; (V) Data analysis and interpretation: V Lucas-Cava, F Sun; (VI) Manuscript writing: All authors; (VII) Final approval of manuscript: All authors.

Correspondence to: Vanesa Lucas-Cava. Endoluminal Therapy and Diagnosis Unit, Jesús Usón Minimally Invasive Surgery Centre, Road N-521, km 41.8, 10071 Cáceres, Spain. Email: vlucas@ccmijesususon.com; Francisco Miguel Sánchez-Margallo. Scientific Director, Jesús Usón Minimally Invasive Surgery Centre, Road N-521, km 41.8, 10071 Cáceres, Spain. Email: msanchez@ccmijesususon.com.

Background: Prostatic artery embolization (PAE) is an alternative treatment for symptomatic benign prostatic hyperplasia (BPH) in men. A technical modification of conventional PAE has been developed in a canine prostate model consisting of prostatic artery occlusion (PAO) using Onyx® whose therapeutic effect is prostate shrinkage. However, the underlying mechanisms are not well clarified. The purpose was to evaluate the biological mechanisms responsible for therapeutic effects of PAO in the canine prostate.

Methods: Ten adult male beagles (5.0±0.82 years) underwent PAO with Onyx-18 (n=7) and prostatic artery angiography as control (n=3). Blood samples were taken at different time points of follow-up (baseline, 1 week, 2 weeks, 1 month, 3 months and 6 months) to measure the serum canine prostate specific esterase (CPSE). MRI examinations were also performed to document the prostate volume (PV) before and after interventions at different time points of follow-up. Prostates were harvested at 2 weeks (n=2) in the PAO-group, and the remaining ones (n=8) at 6 months for the determinations of intraprostatic testosterone and dihydrotestosterone (DHT) by ELISA, apoptosis by TUNEL assay and histopathological study.

Results: The mean serum CPSE concentration started to decrease significantly from 2 weeks to 6 months after PAO along with PV compared with baseline data. In addition, a moderate but significant correlation was observed between CPSE and PV (r=0.655, P=0.000). Regarding intraprostatic androgens, testosterone was significantly higher after PAO than control (19.70 *vs.* 4.87 ng/mL, P=0.002), whereas DHT was lower but no significant (112.52 *vs.* 138.35 pg/mL, P=0.144). In histological study, PAO induced a severe hemorrhagic necrosis in the whole prostates along with inflammatory cell infiltration at early 2 weeks, and then diffuse interstitial fibrosis with atrophy of the glandular epithelium and intraprostatic cavity formation at 6 months. Apoptosis was detected in all specimens with higher apoptotic index after PAO at 2 weeks (7.35%) and at 6 months (4.38%) compared with control (2.64%), without statistically significant difference between groups.

^ ORCID: Vanesa Lucas-Cava, 0000-0002-9807-386X; Francisco Miguel Sánchez-Margallo, 0000-0003-2138-988X; Beatriz Moreno-Lobato, 0000-0001-5091-9718; Juan Rafael Lima-Rodríguez, 0000-0003-3710-6936; Virginio García-Martínez, 0000-0002-7760-1985; Carmen López-Sánchez, 0000-0003-3296-2071; Fei Sun, 0000-0002-3865-3811.

Conclusions: PAO induces hemorrhagic ischemia predominantly resulting in necrosis rather than apoptosis with prostate shrinkage. CPSE is a potential biomarker to assess the response to PAO in the canine prostate.

Keywords: Apoptosis; embolization; benign prostatic hyperplasia (BPH); canine model; pathology

Introduction

Benign prostatic hyperplasia (BPH) is a common disease in men with a reported prevalence at 50% of men in their 50s and 80% in the seventh decade (1). BPH is characterized by an increased number of epithelial and stromal cells in the periurethral area of the prostate in men causing lower urinary tract symptoms (LUTS). The etiology is multifactorial owing to a disorder related to hormones, growth factors, and programmed cell death leading to cellular accumulation and then prostate growth (2). At present, treatments for LUTS secondary to BPH (LUTS/BPH) are targeted at different underlying mechanisms involved in the BPH development.

Prostatic artery embolization (PAE) is an emerging interventional technique that has recently gained in popularity worldwide to treat moderate to severe LUTS/BPH with improvements in urological symptoms and relatively fewer adverse events (3,4). The rationale of PAE is the shrinkage of the enlarged prostate by devascularization of the gland tissue, which induces prostatic ischemia, and consequently a prostate volume (PV) reduction. Apart from ischemic injury, other proposed mechanisms behind PAE included the deprivation of androgens by blockage of the circulation and prostate apoptosis (5). Previous animal experiments have demonstrated that the decrease of androgens after castration or antiandrogen therapy may induce a prostate shrinkage by apoptosis (6,7). Likewise, medical treatment for BPH, such as the use of 5α-reductase inhibitors (finasteride), has also shown the apoptosis of prostatic epithelial cells leading to prostate size reduction both in men and dogs (8,9). The depletion of androgen effects by different targeted therapies has confirmed its effectiveness on prostate involution. Based on this rationale, a new technical modification of the conventional PAE has been developed in a canine model, involving the prostatic artery occlusion (PAO) at the level of its trunk and main branches with a liquid embolic agent in an attempt to induce

ischemia and then prostate shrinkage. The CIRSE standard of practice on PAE recommends imaging examination to evaluate prostate shrinkage (10). However, there are other tools, such as prostate-specific antigen (PSA) which has demonstrated to be an effective biomarker to predict and assess the PV reduction after PAE (11). Its counterpart in dogs is canine prostatic specific esterase (CPSE) whose level is related with PV, and then is used as biomarker in the veterinary diagnosis of canine BPH and other prostatic diseases (12-14).

To elucidate the likely underlying mechanism of PAO, the assessment of intraprostatic hormones, biomarker, and apoptosis was performed in the canine prostate with the purpose to evaluate the pathophysiological changes induced by PAO. The following article was presented in accordance with the ARRIVE reporting checklist (available at https://tau.amegroups.com/article/view/10.21037/tau-22-423/rc).

Methods

Animals

Experiments were performed under a project license (No. 2019209010000930) granted by Regional Ethics Committee of Junta de Extremadura, in compliance with Spanish national guidelines for the care and use of animals. Ten adult male Beagle dogs were enrolled in this study (15.50±4.09 kg; 5.00±0.82 years) with at least a prostate size larger than 12 mL. Three dogs underwent prostatic artery angiography as sham procedure in the control group, and 7 dogs underwent PAO in the experimental group, in which 2 dogs were euthanized at 2 weeks after PAO, and the remaining animals at 6 months after procedures.

PAO procedure

Under general anesthesia and sterile conditions, vascular access in the femoral artery was established percutaneously.

The prostatic artery was catheterized using a coaxial system with a 2.4 Fr microcatheter (Progreat, Terumo Medical, Somerset, NJ, USA) with a 0.016" microwire (GT, Terumo Medical, Somerset, NJ, USA). The microcatheter tip was placed inside of the main trunk of the prostatic artery, and superselective angiography was performed by manual injection of diluted contrast medium (Omnipaque 240 ng I/mL, GE Healthcare, Madrid, Spain) in all animals. In the experimental group, ethylene-vinyl alcohol copolymer (EVOH) (Onyx®-18 /ev3 Micro Therapeutic Inc., Irvine, CA, USA) was then administrated according to manufacturer's instruction until achieving the occlusion of the prostatic artery and its main branches. Control angiography in the internal iliac artery was conducted to document the technical success of complete occlusion of the targeted arteries in PAO-group. The procedure was repeated subsequently on the contralateral side with the same protocol in both groups. At the end of the intervention, the animals were recovered and maintained in animal housing with analgesic (buprenorphine) for 3 days, and antibiotic (amoxicillin) and anti-inflammatory (meloxicam) for 1 week.

In addition, follow-up angiography was performed at the end of study following the protocol described above to document the recanalization of occluded prostatic arteries in all dogs.

Image evaluation

All dogs under general anesthesia underwent MRI evaluation with a 1.5T system (Intera; Philips Medical Systems, Best, The Netherlands) at different time points, including before the angiographic procedure as baseline data, and at 1 week, 2 weeks, 1 month, 3 months and 6 months after the procedure as the endpoint of study. MRI examination included T1-weighted turbo spin-echo and T2-weighted turbo spin-echo images in axial, coronal and sagittal planes. The PV was measured on T2-weighted images with OsiriX 64-bit software (Pixmeo, Bernex, Switzerland).

Blood extraction

Blood samples were collected from the saphenous vein into vacuum tubes without anticoagulant at 9–10 a.m. at the same different time points of follow-up (baseline, 1 week, 2 weeks, 1 month, 3 months and 6 months). Blood samples were allowed to clot at room temperature and then centrifuged for serum separation at 3,500 rpm for 15 minutes. The serum was stored in a freezer at –80 ℃ until analysis.

Postmortem study

At the end of the study, all animals were euthanized under general anesthesia with an overdose of potassium chloride and subjected to necropsy. The prostate and surrounding organs such as urinary bladder, rectum, and vas deferens were carefully inspected. The prostate was harvested and sectioned axially into four blocks, two of which were fixed in 4% paraformaldehyde for 48–72 h at 4 ℃ for microscopy study, and the other two were stored in a freezer at –80 ℃ for the determination of androgen concentration in tissue. The prostate specimens were dehydrated in a graded series of ethanol and embedded in paraffin. Sections were cut into 7 μm thickness for hematoxylin and eosin (H&E) and immunohistochemical staining.

Hormone and biomarker assays

Canine testosterone was measured using a solid phase sandwich ELISA method [Canine Testosterone (T) ELISAN Kit, CUSABIO, Wuhan Hi-tech Medical Devices Park, Wuhan, Hubei Province, China]. The sensitivity of the testosterone kit was 0.05 ng/mL. For canine DTH measurement, a solid phase sandwich ELISA method was used [Canine Dihydrotestosterone (DHT) ELISAN Kit, CUSABIO, Wuhan Hi-tech Medical Devices Park, Wuhan, Hubei Province, China]. The sensitivity of the DHT kit was 20 pg/mL. Both ELISA kits were used to analyze intraprostatic canine testosterone and DHT concentrations. Prostates were defrosted at room temperature and then cut into 100 mg which was homogenized manually in 1 mL PBS 1X. The homogenates were centrifuged at 5,000 g for 5 minutes. The supernatant was removed and assayed immediately for intraprostatic androgen determination. Both procedures were the same where the standards and samples were added to the appropriate microtiter plate wells in duplicate with an antibody specific for each androgen and horseradish peroxidase (HRP) conjugated, then were incubated at 37 ℃ for 1 h. After washing, a substrate solution was added to the wells and incubated at 37 ℃ for 15 minutes in dark. The reaction was stopped, and the optical density of each sample was read at 450 nm. The color was developed in opposite to the amount of androgen concentration in the sample. Testosterone and DHT

Transl Androl Urol 2022;11(12):1655-1666 | https://dx.doi.org/10.21037/tau-22-423

concentrations were calculated based on the standard curve plotted with standard concentrations using CurveExpert 1.4 software.

CPSE was measured by a quantitative enzyme-linked immunosorbent assay (ELISA) type immunoassay on microwell using a commercial dog-specific kit (Odelis CPSE, Virbac BVT, France). Briefly, various calibrator solutions (20, 10, 5.0, 2.5 and 0.0 ng/mL) and control (5.4 ng/mL) were prepared to define the standard curve. All samples were diluted at 1:10 and incubated in duplicate at 37 ℃ for 1 h. After washing, the bound proteins are recognized by HRP conjugate, and incubated again at 37 ℃ for 1 h. After another washing cycle, the colorimetric reaction is generated by the addition of a substrate of HRP for 10 min at room temperature in dark, and then the reaction was stopped. The optical density of each sample was read at 450 nm, and CPSE concentrations were calculated based on the standard curve plotted with calibrator concentrations.

Apoptosis assay

Formalin-fixed paraffin-embedded prostates were used to detect apoptotic cells by TUNEL (TdT-mediated dUTP Nick End Labeling) using the ApopTag Plus Peroxidase In Situ Apoptosis Detection Kit (Millipore Corporation-California). The assays were conducted following the manufacturer's instructions. Briefly, the prostate sections were dewaxed, hydrated, and treated with proteinase K (20 μg/mL) at room temperature for 15 min. After washing, endogenous peroxidase activity was quenched with a 3% hydrogen peroxide solution for 5 min. Each section was incubated with equilibration buffer, and then with working strength terminal deoxynucleotidyl transferase (TdT) enzyme diluted 30% in reaction buffer at 37 ℃ for 1 h in a humidified chamber. The sections were agitated in strength stop/wash buffer in a jar for 15 sec, and then incubated for 10 min at room temperature. Slides were washed in PBS and incubated with antidigoxigenin peroxidase conjugate for 30 min in a humidified chamber at room temperature. After washing, reaction occurred by addition of substrate with diaminobenzidine (DAB) diluted 1:50 in DAB dilution buffer with development of color for 3 minutes at room temperature. After washing in distilled water, sections were counterstained with hematoxylin. Apoptosis was measured by the apoptotic index calculated as the mean percentage of TUNEL-positive cells divided by the total number of prostatic cells in ten random and non-contiguous sections at 1,000× of magnification.

Statistical analysis

The statistical analysis was conducted with SPSS version 24. The descriptive analysis was performed in all variables and expressed as means ± standard deviation. The normality study was checked using the Shapiro-Wilk test. The independent sample t-test was used to compare the differences between groups, and paired sample t-test for differences at different time points of follow-up. Pearson's rank correlation was used to estimate the relationship between PV and CPSE concentration. $P<0.05$ was considered to indicate a statistically significant difference.

Results

Image evaluation

There was no significant difference concerning the mean PV at baseline between groups (control, 17.16 mL *vs.* PAO, 17.00 mL). In animals of PAO group, the mean PV started to decrease significantly at 2 weeks compared to baseline data with a mean reduction rate of 50.47% at 6 months of follow-up (8.42 mL, $P=0.001$). However, in animals of control group, decrease in PV was also detected with a mean PV reduction rate of 20.10% during 6 months follow-up but no significant regarding baseline data (13.71 mL, $P=0.72$). On the other hand, significant differences in the mean PV were noticed at 1 week ($P=0.007$), 1 month ($P=0.019$), 3 months ($P=0.018$) and 6 months ($P=0.05$) of follow-up between groups (*Table 1*).

In follow-up angiography, all animals showed recanalization at least one of occluded prostatic artery at 6 months after PAO, where 3 out of 5 dogs had one reopened prostatic artery whereas the remaining two dogs had both recanalized prostate sides.

Intraprostatic hormone analysis

The mean concentration of intraprostatic testosterone showed a substantial change between groups at the end of the study with higher concentration in PAO-group in comparison with control-group (19.70 *vs.* 4.87 ng/g, $P=0.002$) respectively. However, the mean concentration of intraprostatic DHT was slightly lower after PAO but without statistically significant difference between groups

Table 1 Comparative analysis between prostate volume and serum CPSE concentrations at different time points of follow-up

Follow-up	PV (mL)		P value	CPSE (ng/mL)		P value
	Control	PAO		Control	PAO	
Baseline	17.16±0.13	17.00±3.42	0.566	73.86±46.69	57.90±7.19	0.615
1 week	17.76±0.06	29.02±4.90***	0.007	80.62±71.09	39.6±12.76	0.442
2 weeks	17.05±1.98	11.78±5.17**	0.134	67.22±59.98	14.96±9.86**	0.266
1 month	14.16±3.34	7.41±3.26***	0.019	57.09±8.93	8.93±4.30**	0.134
3 months	15.30±3.03	7.83±3.86***	0.018	46.71±44.13*	14.20±3.11***	0.317
6 months	13.71±0.55	8.42±3.75***	0.050	44.46±41.57*	10.87±3.47***	0.296

*, P value <0.05, **, P value <0.01, ***, P value <0.001 regarding baseline data in each group. P value column corresponds to differences between groups (control *vs.* PAO). CPSE, canine prostate specific esterase; PV, prostate volume; PAO, prostatic artery occlusion.

Table 2 Data of intraprostatic hormone concentrations and apoptosis induced by PAO compared with control at 6-month of follow-up

Measure	Control (n=3)	PAO (n=5)	P value
Testosterone (ng/g)	4.87±1.76	19.70±0.83	0.002
DHT (pg/g)	138.35±18.93	112.52±22.97	0.144
TUNEL index (%)	2.64±0.97	4.38±2.77 (7.35±4.73)	0.253

Data between parentheses is the TUNEL index at 2 weeks of follow-up in PAO-group. PAO, prostatic artery occlusion; DHT, dihydrotestonerone.

(PAO-group, 112.52 pg/g *vs.* Control-group, 138.35 pg/g, P=0.144) (*Table 2*).

CPSE

No statistically significant difference was found in the mean CPSE concentration at baseline between the control and PAO groups (73.86 *vs.* 57.90 ng/mL, P=0.615) respectively. After PAO, the mean CPSE concentration decreased significantly from 2 weeks to 6 months compared with baseline data (*Table 1*). In addition, the comparative analysis between PV and serum CPSE (*Figure 1A*) demonstrated a moderate correlation (r=0.655, P=0.000) (*Figure 1B*).

Postmortem study

In the macroscopic study, the prostate and surrounding organs were visually normal in the control group without changes in the appearance, with a soft consistency due to the glandular content. However, hemorrhage was observed in the rectum wall in one dog, and in the bladder wall with fat adherences in another one at 2 weeks after PAO. In these

animals, the prostates also showed extensive bright and dark areas corresponding to hemorrhagic infarcts with a friable consistency; whereas at 6 months after PAO, prostates displayed a smaller size with cavity formation on one or both lobes along with small areas of glandular tissue of soft consistency mixed with non-glandular zones of fibrous consistency (*Figure 2A*). These findings were histologically observed (*Figure 2B,2C*) where the prostates showed mainly diffuse interstitial fibrosis with lack of glandular architecture and surrogated by connective tissue mixed with foci of atrophic glandular epithelium. The EVOH cast was found in capsular arteries along the lateral border of the prostate without penetration inside the prostate gland (*Figure 2D,2E*); whereas at 2 weeks, PAO induced extensive hemorrhagic necrosis areas (*Figure 3A,3B*) with inflammatory cell (neutrophils) infiltration at 2 weeks of follow-up (*Figure 3C*). In the control group, prostates displayed the typical histopathological features of BPH, including glandular hyperplasia with an increased amount of secretory epithelium mixed with variable amount of stromal tissue (*Figure 4A,4B*). In addition, a complex hyperplasia pattern was also identified with dilated and cystic alveoli
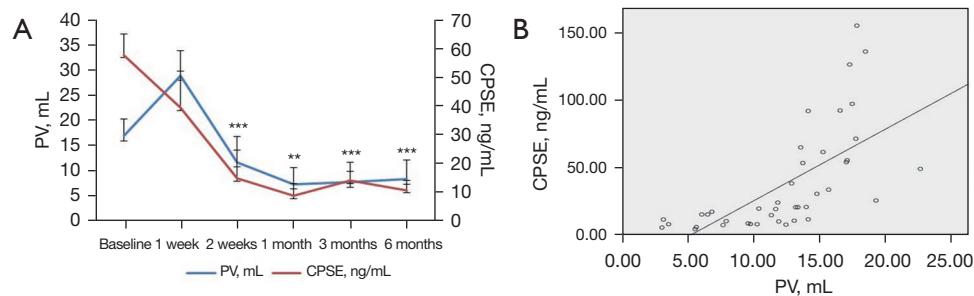
Figure 1 Comparative analysis between prostate volume and serum CPSE concentrations at different time points of follow-up. (A) Changes in PV and CPSE at different time points of follow-up after PAO. Note the statistically significant direct relationship between PV and serum CPSE from 2 weeks to 6 months after PAO except at 1 week due to an increase of PV induced by prostate ischemia along with severe inflammation. (B) The moderate correlation between PV and CPSE (r=0.655, P=0.000). **, P<0.01; ***, P<0.001. PV, prostate volume; CPSE, canine prostate specific esterase; PAO, prostatic artery occlusion.

mixed with multifocal foci of atrophic epithelium and increased stroma (*Figure 4C*).

Apoptosis assay

TUNEL-positive cells were identified based on their brown-stained nuclei, and detected in all dogs. The apoptotic index was higher after PAO in comparison with the control group at 6 months follow-up (4.38% *vs.* 2.64%) respectively; similarly, an increase of TUNEL-positive cells at 2 weeks after PAO was noticed with the highest apoptotic index of 10.69%. No statistically significant differences were identified either between groups or at different time points at follow-up (*Figure 5A-5C*).

Discussion

PAO in the present study led to shrinkage of the treated prostate with two major proposed mechanisms, creation of the global ischemia and blockage of the androgens circulation to the prostate. PAE-induced ischemia with subsequent necrosis and the secondary prostate shrinkage has been well described in clinical practice and animal experiments (5,15,16). In the recent years, some technical modifications of the original PAE have been developed in an attempt to improve its effectiveness and safety in patients, such as the PErFecTED technique (Proximal Embolization First, Then Embolize Distal) which led to greater infarcts in prostates attributable to a better distribution and delivery of embolic agent in the targeted prostatic arteries (17); but no significant difference regarding PV reduction was found between both techniques (18). The use of coil as adjunctive

treatment in PAE has been also developed with aiming to increase the effectiveness in PAE delivering a coil into the main prostatic arteries after PAE (19); and its safety occluding anastomosis between the prostatic artery and adjacent organs (bladder, penis or rectum) avoiding non-target embolization during the particle embolization (20). Even liquid embolic agent (glue) has been described in PAE without significant differences in International Prostate Symptoms Score, quality of life and PV compared with microparticles in patients (21,22). The conventional PAE using microparticles achieves a peripheral embolization of intraprostatic vasculature inducing a local prostate ischemia, whereas PAO involves the occlusion of the prostatic artery and its main branches with a liquid embolic agent, resulting in the global prostate ischemia in canine model (23). However, the underlying mechanisms to the PAO-induced ischemia are unknown. In addition, the complete occlusion of the prostatic artery might have more benefits in blockage of the androgens circulation to the prostate compared with PAE, thus inducing the hormone-related prostate apoptosis with an enhanced effect on the prostate shrinkage. So, the evaluation of the pathological response to PAO may lend weight to the assumption of the mechanisms behind PAE.

Our findings indicated that PAO substantially reduced PV from 2 weeks when compared with baseline data (11.78 mL *vs.* baseline 17.00 mL, P<0.05), with the maximal reduction rate at 1 month (7.41±3.26, P<0.01), and this PV reduction was still significant at 3 months (7.83±3.86, P<0.01) and 6 months (8.42±3.75, P<0.01), highlighting the durability of therapeutic effect after PAO. The PV reduction was significant at 1, 3 and 6 months after PAO compared with control group; although these animals also showed a
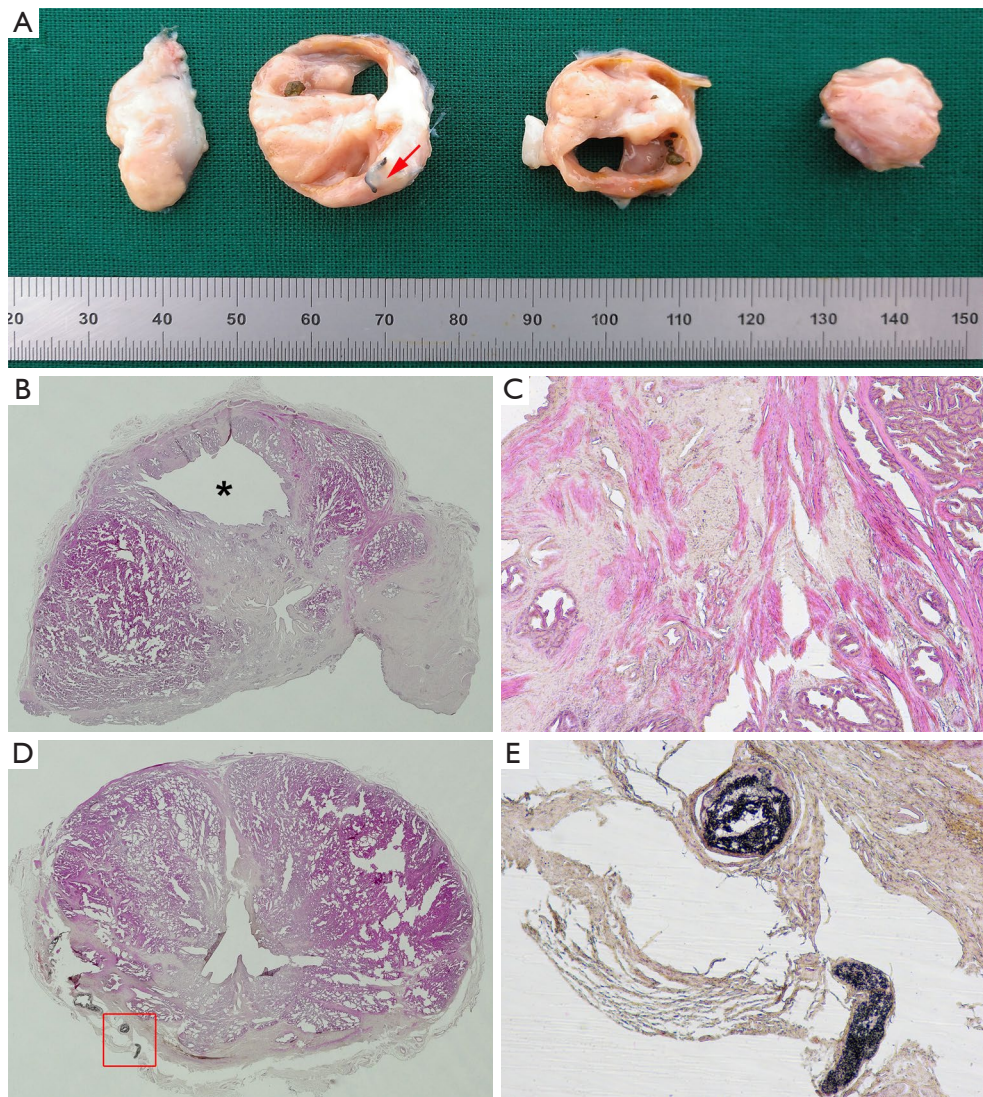
Figure 2 Histopathological findings in the prostate at 6 months after PAO (Hematoxilin & Eosin staining). Macroscopy study (A) shows cavity formation in both prostate sides. Note the cast of EVOH in the peripheral gland (red arrow). Microscopy study (B-E) reveals intraprostatic cavity formation (asterisk in B) and diffuse interstitial fibrosis with foci of the glandular epithelium (magnified view 40× in C). Note EVOH cast was found in the prostate capsular artery (square portion in D and its magnified view 40× in E). PAO, prostatic artery occlusion; EVOH, ethylene-vinyl alcohol copolymer.

decrease in PV but no significant at the same time points of follow-up, perhaps due to the prostatic artery catheterization during the follow-up angiography which would have been able to induce a little spasm, and subsequent a little decrease of PV. However, it is worth noting that the mean PV at one week after PAO significantly increased (+70.71%) compared with the baseline data due to hemorrhagic infarct along with severe inflammation induced by PAO which caused tissue swelling at this stage. Of note, previous studies on

PAE in dogs by Lucas-Cava *et al.* (16,24) demonstrated that there was a slight decrease in the mean PV at 1 week after PAE, from –2.4% to –9.07%. The inconsistency suggested that PAO induced a global ischemia of the prostate with severe secondary inflammatory reaction and massive edema increasing the PV in the acute phase; whereas PAE led to local ischemia with less inflammatory reaction. Our histopathological study revealed extensive hemorrhagic necrosis lesions with intensive inflammatory cell infiltration
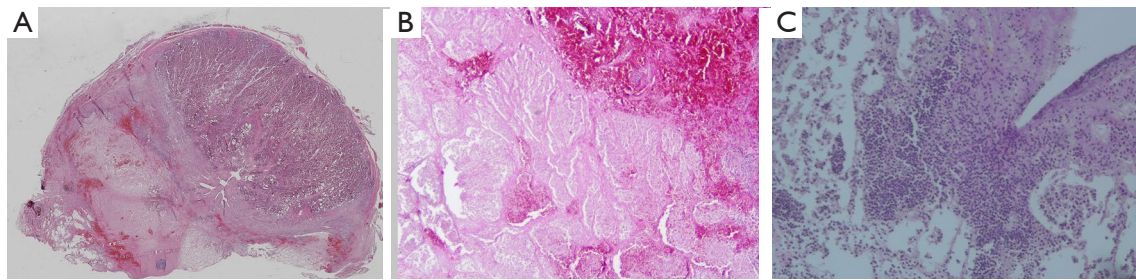
Figure 3 Histopathological findings in the prostate at 2 weeks after PAO (Hematoxilin & Eosin staining). Haemorrhagic necrosis mixed with glandular epithelium (A) was found inflammatory cell infiltration (magnified view 40× in B and C, respectively). PAO, prostatic artery occlusion.
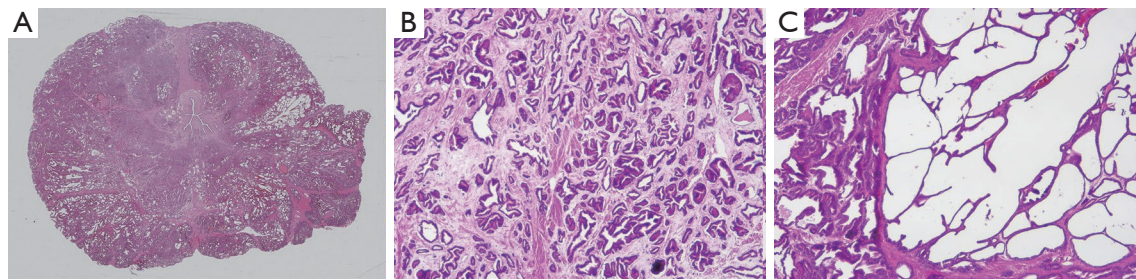

Figure 4 Histopathological findings in the prostate at 6 months after the sham procedure (Hematoxilin & Eosin staining). In the prostates form of the control group, the histopathological features of BPH were observed (A), consisting of glandular epithelium hyperplasia with an increase of alveoli and stromal tissue (magnified view 40× in B). Note dilated and cystic alveoli mixed with multifocal foci of atrophic epithelium typical in the complex form of canine BPH (magnified view 4× in C). BPH, benign prostatic hyperplasia.
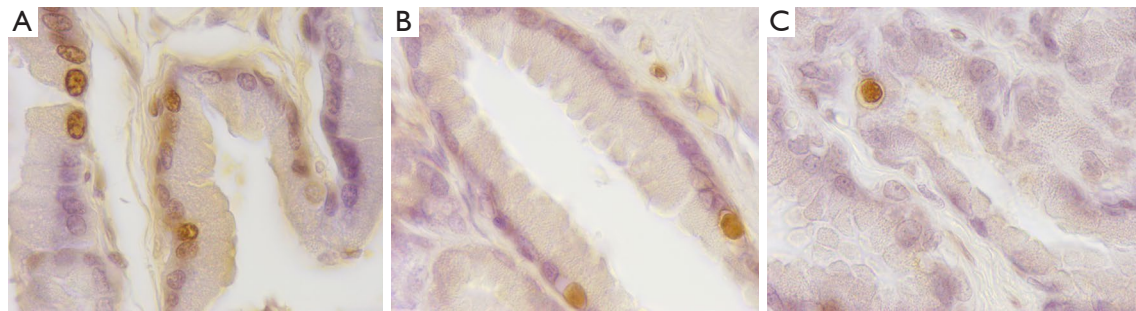

Figure 5 TUNEL assay. Apoptotic cells were identified as brown-stained cells in all specimens mainly in the glandular epithelium counterstained with hematoxylin (magnification view 1,000×). Note the higher TUNEL-positive cells at 2 weeks after PAO (A) regarding 6 months in the PAO-group (B) and the control-group (C). PAO, prostatic artery occlusion.

in the prostates at 2 weeks after PAO, supporting the above assumption. Furthermore, the histopathological study on the specimens at 6 months showed that the scarring of the prostate infarction resulted in the shrinkage of the treated prostate, where the ischemic necrosis was replaced by interstitial fibrosis with presence of glandular cysts and epithelial atrophy or cavity lesions.

Besides necrosis after PAO, apoptosis might be another important pathway resulting in atrophy and prostate shrinkage. Current evidence indicates that the pathway

of cell death (necrosis or apoptosis) induced by hypoxia/ischemia depends on its degree and duration. Persistent or severe ischemia lead to depletion of generation of cellular energy in ATP, and consequently leading to failure of many energy-dependent metabolic pathways, and cell death occurs by necrosis (25). By contrast, when ischemia is less severe and more gradual, cells die by apoptosis with DNA fragmentation and formation of apoptotic bodies as the last step (26). In a transient ischemia study of the rat prostate (27), a threefold increase in the volume density of apoptotic epithelial cells was detected; furthermore, the relative increase in apoptosis was not abolished by the administration of testosterone, suggesting the underlying androgen-independent mechanism of ischemia was partly involved.

Androgen-related prostate apoptosis is another issue of interest in both preliminary studies and clinical trials. It is well known that the hormonal regulation of androgens plays a critical role in the homeostasis of the prostate. When the supply of circulating androgens is depleted by castration therapies, or androgen action is blocked by the 5α-reductase inhibitors, the prostatic cells die by apoptosis (5,28-30). The decrease of the growth potential of prostatic cells caused by the lack of androgens along with the extensive loss of cells by apoptotic pathway contributes to the shrinkage or regression of prostatic tissue (29). It should be noted that ischemia-induced prostate apoptosis occurs at the early phase of hypoxic insult, which was observed at its peak on days 3–6 and lasted until days 10–15 in rodent castrated models (6,28), whereas androgen-related prostate apoptosis was a relatively longer-term effect, with a significant shrinkage of the enlarged prostate typically observed at 6 months after finasteride therapy in patients with BPH (8,30). Therefore, the timing for the TUNEL assay to detect apoptotic cells is critical. In our study, the TUNEL assay was conducted in animals at 2 weeks and 6 months after PAO. In animals of the control-group, the mean apoptosis index was identified as 2.64%; whereas a higher apoptosis index was observed at 2 weeks (7.35%) and 6 months (4.38%) in animals after PAO. Although no statistically significant difference was found between groups and at different time points possibly due to the small sample size in this study, the data suggested that more apoptotic cells were induced at 2 weeks caused by ischemia and the relatively more apoptosis could be attributable to the decrease in the intraprostatic DHT levels at 6 months after PAO. It has been reported that up to 40% of apoptotic cells in the canine prostate were induced by surgical castration from day 7 to 14 (31,32), which was

much higher than our findings at 2 weeks. This was because in the castrated prostate the only cell death observed was in the form of apoptosis and oncosis; whereas, in our animals, substantial necrosis occurred in the prostate with small areas of the residual gland tissue where the apoptotic cells were identified. Therefore, the pathological findings at 2 weeks after PAO in the present study demonstrated that PAO in the canine prostate predominantly resulted in extensive necrosis rather than prostate apoptosis, which is mainly observed in the residual gland tissue nearby the necrosis lesions.

It is interesting to note that the findings of the high intraprostatic levels of androgens at 6 months were out of expectation. It was hypothesized that PAO in the present study might block the circulation of testosterone and DHT in the treated prostate by occlusion of the prostatic artery with a liquid permanent embolic agent, thus achieving an "intraprostatic castration effect" to enhance the prostate apoptosis (33). However, the mean intraprostatic DHT level was lower but not significant at 6 months after PAO (PAO, 112.52 ± 22.97 pg/mL, *vs.* Control, 138.35 ± 18.93 pg/mL, P=0.144); conversely, the mean intraprostatic testosterone level significantly increased (PAO, 19.70 ± 0.83 ng/mL *vs.* Control, 4.87 ± 1.76 ng/mL, P=0.002) in comparison to animals in control-group. One possible reason was the recanalization of the occluded prostatic arteries, since in the follow-up angiography at 6 months after PAO, at least one of the treated prostatic arteries were identified with partial or complete recanalization in all dogs. Despite Onyx® is considered as permanent embolic agent; the presence of recanalization is related with the incomplete filled of the embolized vessels leading to spaces inside of the lumen where recanalization started (34). Another reason might be that PAO resulted in the destruction of most gland tissue with massive fibrosis, cavity formation, and atrophy in the prostate, and therefore the enzyme activity of 5α-reductase greatly decreased in the residual epithelium and stroma tissue in the prostate. In a report by Zhao *et al.* was observed an increase in serum and intra-prostatic testosterone levels accompanied by a decrease in DHT levels after treatment with two different kinds of 5α reductase inhibitors. In both cases, there was no conversion of testosterone into DHT with an accumulation of testosterone in blood and tissue (35). Similarly, this might partially explain the significant higher testosterone level by accumulation inside of prostate at 6 months after PAO due to a prostate recanalization along with relatively lower intraprostatic DHT level by destruction of prostate tissue.

PSA is a commonly used biomarker for BPH patients.

Ever since Roehrborn *et al.* reported a strong age-dependent relationship between serum PSA level and PV in a large cohort of men with BPH (36), PSA as a surrogate of PV has been investigated and confirmed its predictive role for assessing future prostate growth, risk of BPH progression, and monitoring the response to therapy (37). In clinical practice of PAE, PSA is tested as a parameter to evaluate clinical response. A significant relationship between the serum PSA level at 24 hours after PAE and subsequent relief in LUTS has been validated, indicating that PSA is a potential clinical predictor (38). However, PSA is not detected in canine blood or seminal fluid; instead, CPSE as its counterpart is identified in canine serum and seminal fluid (12). CPSE is a trypsin-like enzyme secreted by the prostatic epithelial cells mainly in the apical region of the canine prostate, which can be inhibited by antiandrogen treatment or surgical castration (13,39). Currently, CPSE has been used in the veterinary diagnosis of canine BPH and other prostatic diseases, with a significant positive correlation between CPSE level and PV (r=0.448, P<0.001) (13,14). This is in agreement with our findings of a moderate correlation between CPSE level and PV (r=0.655, P=0.00). More importantly, our findings showed a significant decrease in the mean CPSE levels at 2 weeks, 1, 3 and 6 months after PAO when compared with baseline data, which was in accordance with the reduction in PV observed at each time point. Similar to PSA in PAE in human patients, the decrease in CPSE after PAO can be explained by the destruction of the prostate glandular tissue induced by intervention, suggesting CPSE can be used as a new measure to evaluate therapeutic response in preclinical studies on both PAO and PAE in dogs.

The main limitations in this study were the small sample size between groups and prostate recanalization. The former, a greater number of animals in the different groups could achieve to detect statistically significant differences at long-term. The latter, the new inflow of blood into the prostate might have mimicked the effect of PAO on prostate. Additionally, the testing of CPSE levels at 24–48 hours after PAO would have been interesting in an attempt to evaluate its predictive role of subsequent technical effectiveness of PAO.

Conclusions

PAO with Onyx® successfully results in the prostate shrinkage mainly through ischemia-induced tissue necrosis and consequent gland fibrosis and atrophy with less

effect on apoptosis in a canine model. Due to the high rate of recanalization of the occluded arteries, androgen-related prostate apoptosis at the late stage was minimal in comparison with the acute ischemic apoptosis. CPSE is a promising biomarker in future preclinical studies for monitoring the PV changes in response to new minimally invasive techniques in canine models. Further studies with a large sample size are needed, as well as elucidating the underlying mechanism behind prostate recanalization and how might affect the therapeutic effect of PAO.

Footnote

Reporting Checklist: The authors have completed the ARRIVE reporting checklist (available at https://tau.amegroups.com/article/view/10.21037/tau-22-423/rc).

Data Sharing Statement: Available at https://tau.amegroups.com/article/view/10.21037/tau-22-423/dss

Conflicts of Interest: All authors have completed the ICMJE uniform disclosure form (available at https://tau.amegroups.com/article/view/10.21037/tau-22-423/coif). All authors report that this study was supported by grants IB18129 and GR 21201 from Plan Regional de Investigación, Consejería de Economía, Ciencia y Agenda Digital, Junta de Extremadura, and Fondo Europeo de Desarrollo Regional. The authors have no other conflicts of interest to declare.

Ethical Statement: The authors are accountable for all aspects of the work in ensuring that questions related to the accuracy or integrity of any part of the work are appropriately investigated and resolved. Experiments were performed under a project license (No. 2019209010000930) granted by Regional Ethics Committee of Junta de Extremadura, in compliance with Spanish national guidelines for the care and use of animals.

Transl Androl Urol 2022;11(12):1655-1666 | https://dx.doi.org/10.21037/tau-22-423

References

1. Egan KB. The Epidemiology of Benign Prostatic Hyperplasia Associated with Lower Urinary Tract Symptoms: Prevalence and Incident Rates. Urol Clin North Am 2016;43:289-97.

2. Sun F, Crisóstomo V, Báez-Díaz C, et al. Prostatic Artery Embolization (PAE) for Symptomatic Benign Prostatic Hyperplasia (BPH): Part 1, Pathological Background and Clinical Implications. Cardiovasc Intervent Radiol 2016;39:1-7.

3. McWilliams JP, Bilhim TA, Carnevale FC, et al. Society of Interventional Radiology Multisociety Consensus Position Statement on Prostatic Artery Embolization for Treatment of Lower Urinary Tract Symptoms Attributed to Benign Prostatic Hyperplasia: From the Society of Interventional Radiology, the Cardiovascular and Interventional Radiological Society of Europe, Société Française de Radiologie, and the British Society of Interventional Radiology: Endorsed by the Asia Pacific Society of Cardiovascular and Interventional Radiology, Canadian Association for Interventional Radiology, Chinese College of Interventionalists, Interventional Radiology Society of Australasia, Japanese Society of Interventional Radiology, and Korean Society of Interventional Radiology. J Vasc Interv Radiol 2019;30:627-37.e1.

4. Ray AF, Powell J, Speakman MJ, et al. Efficacy and safety of prostate artery embolization for benign prostatic hyperplasia: an observational study and propensity-matched comparison with transurethral resection of the prostate (the UK-ROPE study). BJU Int 2018;122:270-82.

5. Sun F, Crisóstomo V, Báez-Díaz C, et al. Prostatic Artery Embolization (PAE) for Symptomatic Benign Prostatic Hyperplasia (BPH): Part 2, Insights into the Technical Rationale. Cardiovasc Intervent Radiol 2016;39:161-9.

6. Banerjee S, Banerjee PP, Brown TR. Castration-induced apoptotic cell death in the Brown Norway rat prostate decreases as a function of age. Endocrinology 2000;141:821-32.

7. Shibata Y, Fukabori Y, Ito K, et al. Comparison of histological compositions and apoptosis in canine spontaneous benign prostatic hyperplasia treated with androgen suppressive agents chlormadinone acetate and finasteride. J Urol 2001;165:289-93.

8. Sutton MT, Yingling M, Vyas A, et al. Finasteride targets prostate vascularity by inducing apoptosis and inhibiting cell adhesion of benign and malignant prostate cells. Prostate 2006;66:1194-202.

9. Lima CB, Angrimani DSR, Flores RB, et al. Endocrine, prostatic vascular, and proapoptotic changes in dogs with benign prostatic hyperplasia treated medically or surgically. Domest Anim Endocrinol 2021;75:106601.

10. Cornelis FH, Bilhim T, Hacking N, et al. CIRSE Standards of Practice on Prostatic Artery Embolisation. Cardiovasc Intervent Radiol 2020;43:176-85.

11. Bilhim T, Pisco J, Pereira JA, et al. Predictors of Clinical Outcome after Prostate Artery Embolization with Spherical and Nonspherical Polyvinyl Alcohol Particles in Patients with Benign Prostatic Hyperplasia. Radiology 2016;281:289-300.

12. Sun F, Báez-Díaz C, Sánchez-Margallo FM. Canine prostate models in preclinical studies of minimally invasive interventions: part II, benign prostatic hyperplasia models. Transl Androl Urol 2017;6:547-55.

13. Alonge S, Melandri M, Aiudi G, et al. Advances in Prostatic Diagnostics in Dogs: The Role of Canine Prostatic Specific Esterase in the Early Diagnosis of Prostatic Disorders. Top Companion Anim Med 2018;33:105-8.

14. Pinheiro D, Machado J, Viegas C, et al. Evaluation of biomarker canine-prostate specific arginine esterase (CPSE) for the diagnosis of benign prostatic hyperplasia. BMC Vet Res 2017;13:76.

15. Wang MQ, Zhang JL, Xin HN, et al. Comparison of Clinical Outcomes of Prostatic Artery Embolization with 50-μm Plus 100-μm Polyvinyl Alcohol (PVA) Particles versus 100-μm PVA Particles Alone: A Prospective Randomized Trial. J Vasc Interv Radiol 2018;29:1694-702.

16. Lucas-Cava V, Sánchez-Margallo FM, García-Martínez V, et al. Prostatic artery embolization: magnetic resonance image (MRI) findings in the early detection of prostate infarction in a canine spontaneous benign prostatic hyperplasia model. Transl Androl Urol 2021;10:869-78.

17. Carnevale FC, Moreira AM, Antunes AA. The "PErFecTED Technique": Proximal Embolization First, Then Embolize Distal for Benign Prostatic Hyperplasia.

Cardiovasc Intervent Radiol 2014;37:1602-5

18. Carnevale FC, Iscaife A, Yoshinaga EM, et al. Transurethral Resection of the Prostate (TURP) Versus Original and PErFecTED Prostate Artery Embolization (PAE) Due to Benign Prostatic Hyperplasia (BPH): Preliminary Results of a Single Center, Prospective, Urodynamic-Controlled Analysis. Cardiovasc Intervent Radiol 2016;39:44-52.

19. Galla N, Maron SZ, Voutsinas N, et al. Adjunctive Coil Embolization of the Prostatic Arteries After Particle Embolization for Prostatic Artery Embolization. Cardiovasc Intervent Radiol 2021;44:1994-8.

20. Bhatia S, Sinha V, Bordegaray M, et al. Role of Coil Embolization during Prostatic Artery Embolization: Incidence, Indications, and Safety Profile. J Vasc Interv Radiol 2017;28:656-64.e3.

21. Loffroy R, Guillen K, Salet E, et al. Prostate Artery Embolization Using N-Butyl Cyanoacrylate Glue for Urinary Tract Symptoms Due to Benign Prostatic Hyperplasia: A Valid Alternative to Microparticles? J Clin Med 2021;10:3161.

22. Salet E, Crombé A, Grenier N, et al. Prostatic Artery Embolization for Benign Prostatic Obstruction: Single-Centre Retrospective Study Comparing Microspheres Versus n-Butyl Cyanoacrylate. Cardiovasc Intervent Radiol 2022;45:814-23.

23. Lucas-Cava V, Sánchez-Margallo FM, Dávila-Gómez L, et al. Prostatic artery occlusion versus prostatic artery embolisation for the management of benign prostatic hyperplasia: early results in a canine model. Br J Radiol 2022;95:20220243.

24. Lucas Cava V, Sánchez Margallo FM, Báez Díaz C, et al. Prostatic artery embolization with polyethylene glycol microspheres: evaluation in a canine spontaneous benign prostatic hyperplasia model. CVIR Endovasc 2020;3:44.

25. Kumar V, Abbas A, Aster J. Cell Injury, Cell Death, and Adaptations. In: Kumar V, Abbas A, Aster J, editors. Robbins Basic Pathology. 10th ed. Philadelphia, Pennsylvania: Elsevier, 2018:31-56.

26. Shabsigh A, Chang DT, Heitjan DF, et al. Rapid reduction in blood flow to the rat ventral prostate gland after castration: preliminary evidence that androgens influence prostate size by regulating blood flow to the prostate gland and prostatic endothelial cell survival. Prostate 1998;36:201-6.

27. Lekås E, Engstrand C, Bergh A, et al. Transient ischemia induces apoptosis in the ventral prostate of the rat. Urol Res 1999;27:174-9.

28. Kwong J, Choi HL, Huang Y, et al. Ultrastructural and biochemical observations on the early changes in apoptotic epithelial cells of the rat prostate induced by castration. Cell Tissue Res 1999;298:123-36.

29. Buttyan R, Ghafar MA, Shabsigh A. The effects of androgen deprivation on the prostate gland: cell death mediated by vascular regression. Curr Opin Urol 2000;10:415-20.

30. Golbano JM, Lóppez-Aparicio P, Recio MN, et al. Finasteride induces apoptosis via Bcl-2, Bcl-xL, Bax and caspase-3 proteins in LNCaP human prostate cancer cell line. Int J Oncol 2008;32:919-24.

31. Niu YJ, Ma TX, Zhang J, et al. Androgen and prostatic stroma. Asian J Androl 2003;5:19-26.

32. Niu Y, Xu Y, Zhang J, et al. Proliferation and differentiation of prostatic stromal cells. BJU Int 2001;87:386-93.

33. Sun F. Clinics in Oncology Prostatic Artery Embolization: A Potential Treatment Option for Localized Prostate Cancer. Clin Oncol 2016;1:1-3.

34. Natarajan SK, Born D, Ghodke B, et al. Histopathological changes in brain arteriovenous malformations after embolization using Onyx or N-butyl cyanoacrylate. Laboratory investigation. J Neurosurg 2009;111:105-13.

35. Zhao XF, Yang Y, Wang W, et al. Effects of competitive and noncompetitive 5α-reductase inhibitors on serum and intra-prostatic androgens in beagle dogs. Chin Med J (Engl) 2013;126:711-5.

36. Roehrborn CG, Boyle P, Gould AL, et al. Serum prostate-specific antigen as a predictor of prostate volume in men with benign prostatic hyperplasia. Urology 1999;53:581-9.

37. Nickel JC. Benign prostatic hyperplasia: does prostate size matter? Rev Urol 2003;5 Suppl 4:S12-7.

38. Sun F, Lucas-Cava V, Sánchez-Margallo FM. Clinical predictive factors in prostatic artery embolization for symptomatic benign prostatic hyperplasia: a comprehensive review. Transl Androl Urol 2020;9:1754-68.

39. Golchin-Rad K, Mogheiseh A, Nazifi S, et al. Changes in the Serum Prostatic Biomarkers During the Treatment of Benign Prostatic Hyperplasia with a 5alpha-reductase Inhibitor: Finasteride. Top Companion Anim Med 2020;38:100405.